Growth of Oriented Thin Films of Intercalated α-Cobalt Hydroxide on Functionalized Au and Si Substrates

Jong Hyeon Lee, Yi Du, and Dermot O'Hare*

Chemistry Research Laboratory, University of Oxford, Mansfield Road, Oxford OX1 3TA, United Kingdom

Received June 23, 2008. Revised Manuscript Received December 11, 2008

Hydrotalcite-like, α-cobalt hydroxides intercalated with either chloride or anthraquinone-2-sulfonate (AQS2) were crystallized on self-assembled monolayers of 11-mercaptoundecanoic acid on gold as well as poly(acrylic acid) functionalized silicon substrates. These novel functional hybrid films were prepared by the direct nucleation and growth onto the substrate from homogeneous using a homogeneous hydrolysis of $CoCl_2$ by hexamethylenetetramine in the presence of either NaCl or sodium anthraquinone-2-sulfonate. The intercalated α-cobalt hydroxide crystallites nucleate these carboxylic functionalized surfaces and grow with a preferred orientation. Electrochemical experiments on AQS2 intercalated α-$Co(OH)_2$ on 11-mercaptoundecanoic acid functionalized Au thin films show that the intercalated AQS2 anions are still redox active within this oriented crystalline film.

Introduction

Layered double hydroxides (LDHs) are a useful class of inorganic host material for the development of the hybrid inorganic−organic materials.[1] For example, they have recently received considerable attention as hosts for the immobilization of biological compounds.[2] To promote their chemical/biological properties, it would be highly desirable to immobilize the hybrid materials as well ordered films on solid substrates. In addition, highly orientated hybrid LDH films could be useful candidate material for developing optical devices,[3] catalysts,[4] and chemical and biosensors.[5] One approach is to utilize organic interfaces such as functional self-assembled monolayers (SAMs) to direct nucleation of the hybrid LDH films. For example, in biomineralization it has been shown that an organic interface can direct the nucleation and growth of many inorganic phases such as calcium carbonate[6] and zinc oxide.[7] Additionally, well-orientated polymeric organic thin films direct the nucleation and growth of orientated zeolite microcrystal arrays.[8]

Recently, organic or polymer-clay/LDH hybrid films have been fabricated by using a layer-by-layer deposition method with exfoliated LDH nanosheets, where the organic and polymer phases are topotactically adsorbed on clay/LDH platelets.[9] The exfoliation of layered materials[10] or a direct synthesis of LDH nanoplatelets by microemulsion[11] have also attracted interest in the field as methods for building new nanostructured materials. Most LDHs intercalated with either chloride, nitrate, perchlorate, or glycine can be exfoliated into unilamellar nanosheets in formamide by mechanical shaking or ultrasonic treatment.[10] However, the delamination process of LDH compounds always required additional mechanical activation resulting in irregular shaped LDH nanoparticles. Previously, in the fabrication of oriented LDH films, several techniques have been reported such as transparent and smooth LDH films by a hydrolysis of LDH/methoxide,[12] the direct synthesis of oriented curved hexagonal films on a substrate,[13] and monolayer assembly of LDH films by ultrasonification.[14] However, there has been no report of the direct growth of oriented hybrid LDH films from either functionalized gold or silicon substrates.

* Corresponding author. E-mail: dermot.ohare@chem.ox.ac.uk. Fax: +44-1865-272690.

(1) (a) Leroux, F.; Besse, J. P. *Chem. Mater.* **2001**, *13*, 3507. (b) Leroux, F.; Taviot-Gueho, C. *J. Mater. Chem.* **2005**, *15*, 3628. (c) Choi, S. J.; Oh, J. M.; Choy, J. H. *J. Mater. Chem.* **2008**, *18*, 615.

(2) (a) Ogawa, M.; Kuroda, K. *Chem. Rev.* **1995**, *95*, 399. (b) Ding, W.; Gu, G.; Zhong, W.; Zang, W. C.; Du, Y. *Chem. Phys. Lett.* **1996**, *262*, 259. (c) Choy, J. H.; Kwak, S. Y.; Jung, Y. J.; Park, J. S. *Angew. Chem., Int. Ed.* **2000**, *39*, 4042.

(3) (a) Mallouk, T. E.; Kim, H. N.; Ollivier, P. J.; Keller, S. W. *Compr., Supramol. Chem.* **1996**, *7*, 189. (b) Venugopal, B. R.; Ravishankar, N.; Perrey, C. R.; Shivakumara, C.; Rajamathi, M. *J. Phys. Chem. B* **2006**, *110*, 772.

(4) (a) Greenwell, H. C.; Jones, W.; Stamires, D. N.; O'Connor, P.; Brady, M. F. *Green Chem.* **2006**, *8*, 1067. (b) Li, L.; Shi, J. *Chem. Commun.* **2008**, 996.

(5) (a) Darder, M; Lopez-Blanco, M.; Aranda, P.; Leroux, F.; Ruiz-Hitzky, E. *Chem. Mater.* **2005**, *17*, 1969. (b) Han, E.; Shan, D.; Xue, H.; Cosnier, S. *Biomacromolecules* **2007**, *8*, 971. (c) Colombari, M.; Ballarin, B.; Carpani, I.; Guadagnini, L.; Mignani, A.; Scavetta, E.; Tonelli, D. *Electroanalysis* **2007**, *19*, 2321.

(6) Aizenberg, J.; Black, A. J.; Whitesides, G. M. *Nature* **1999**, *398*, 495.

(7) Hsu, J. W. P.; Tian, Z. R.; Simmons, N. C.; Matzke, C. M.; Voigt, J. A.; Liu, J. *Nano Lett.* **2005**, *5*, 83.

(8) Lee, J. S.; Lee, Y. J.; Tae, E. L.; Park, Y. S.; Yoon, K. B. *Science* **2003**, *301*, 818.

(9) (a) Ha, Y. H.; Kwon, Y.; Breiner, T.; Chan, E. P.; Tzianetopoulou, T.; Cohen, R. E.; Boyce, M. C.; Thomas, E. L. *Macromolecules* **2005**, *38*, 5170. (b) Podsiadlo, P.; Liu, Z.; Paterson, D.; Messersmith, P. B.; Kotov, N. A. *Adv. Mater.* **2007**, *19*, 949.

(10) (a) Li, L.; Ma, R.; Ebina, Y.; Iyi, N.; Sasaki, T. *Chem. Mater.* **2005**, *17*, 4386. (b) Ma, R.; Takada, K.; Fukuda, K.; Iyi, N.; Bando, Y.; Sasaki, T. *Angew. Chem., Int. Ed.* **2008**, *47*, 86. (c) Ma, R.; Liu, Z.; Takada, K.; Iyi, N.; Bando, Y.; Sasaki, T. *J. Am. Chem. Soc.* **2007**, *129*, 5257. (d) Wu, Q.; Sjastad, A. O.; Vistad, O. B.; Knudsen, K. D.; Roots, J.; Pedersen, J. S.; Norby, P. *J. Mater. Chem.* **2007**, *17*, 965.

(11) (a) Hu, G.; O'Hare, D. *J. Am. Chem. Soc.* **2005**, *127*, 17808. (b) Hu, G.; Wang, N.; O'Hare, D.; Davis, J. Chem. Commun., 2006, 287. (c) Hu, G.; Wang, N.; O'Hare, D.; Davis, J. *J. Mater. Chem.* **2007**, *17*, 2257.

(12) Gardner, E.; Huntoon, K. M.; Pinnavaia, T. J. *Adv. Mater.* **2001**, *13*, 1263.

10.1021/cm802828z CCC: $40.75
Published on Web 02/16/2009

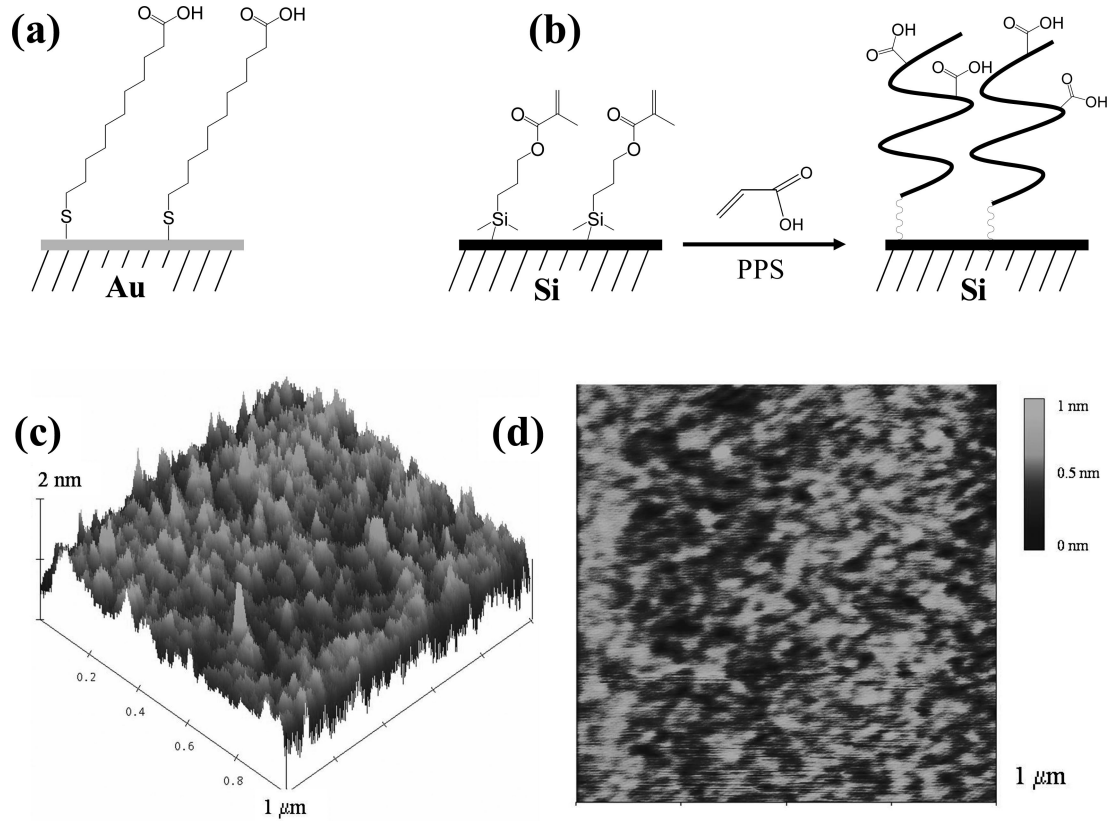

Figure 1. Schematic representation of the organic interfaces of MUA on gold (a) and PAA on TMSPMA/Si substrates (b). AFM images of PAA polymer grown on TMSPMA/Si substrate (c and d).

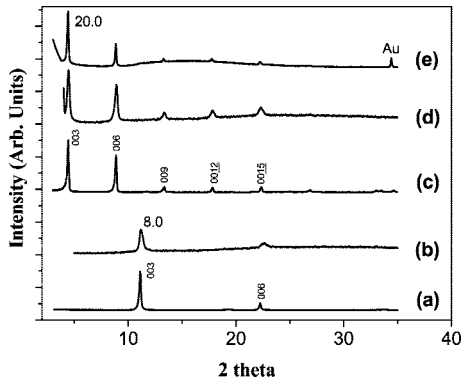

Figure 2. XRD patterns and basal spacings (Å) for (a) microcrystalline Cl-α-$Co(OH)_2$, (b) thin film of Cl-α-$Co(OH)_2$ on PAA/TMSPMA/Si substrate, (c) microcrystalline AQS2-α-$Co(OH)_2$, (d) thin films of AQS2-α-$Co(OH)_2$ on PAA/TMSPMA/Si, and (e) AQS2-α-$Co(OH)_2$ on MUA/Au/Si substrate.

Hydroxides of cobalt are well-known to crystallize in α- and β-polymorphic forms.[15] The α-polymorph is a stoichiometric phase of $Co(OH)_2$ with brucite-like structure, while the α-cobalt hydroxides are hydrotalcite-like compounds consisting of positively charged hydroxide layers and charge-balancing, exchangeable anions such as NO_3^-, Cl^-, AcO^-, SO_4^{2-}, and CO_3^{2-}, in the interlayer gallery between hydroxide layers.[16] α- and β-cobalt hydroxides have been widely studied materials because of their potential application in various fields such as catalysts precursors, nanometer-sized composite materials, and organic-magnetic materials.[17] Moreover, uniform hexagonal platelets of α- and β-cobalt hydroxides were recently synthesized controllably by homogeneous precipitation using hexamethylenetetramine (HMT) as a hydrolysis agent.[18]

In the present study, we investigate the synthesis of novel orientated organic−cobalt hydroxide films on functionalized gold and silicon substrates by employing a homogeneous crystallization technique using HMT. Single oriented monolayers (SAMs) of 11-mercaptoundecanioc acid (MUA) and poly(acrylic acid) (PAA), shown schematically in Figure 1, were used as the organic interfaces and to assist the binding the metal cations on the substrates. A single oriented monolayer of 3-(trimethoxysilyl)propyl methacrylate (TMSPMA) was used as binder for the polymerization which grafts the

(13) (a) Lei, X.; Yang, L.; Zhang, F.; Evans, D. G.; Duan, X. *Chem. Lett.* **2005**, *34*, 1610. (b) Chen, H.; Zhang, F.; Fu, S.; Duan, X. *Adv. Mater.* **2006**, *18*, 3089. (c) Wang, L.; Li, C.; Liu, M.; Evans, D. G.; Duan, X. *Chem. Commun.* **2007**, 123.

(14) (a) Lee, J. H.; Rhee, S. W.; Jung, D. Y. *Chem. Commun.* **2003**, 2740. (b) Lee, J. H.; Rhee, S. W.; Jung, D. Y. *Chem. Mater.* **2004**, *16*, 3774. (c) Lee, J. H.; Rhee, S. W.; Jung, D. Y. *Chem. Mater.* **2006**, *18*, 4740. (d) Lee, J. H.; Rhee, S. W.; Jung, D. Y. *J. Am. Chem. Soc.* **2007**, *129*, 3522.

(15) Oliva, P.; Leonardi, J.; Laurent, J. F.; Delmas, C.; Braconnier, J. J.; Figlarz, M.; Fievet, F. *J. Power Sources* **1982**, *8*, 229.

(16) (a) Portemer, F.; Delahaye-Vidal, A.; Figlarz, M. *J. Electrochem. Soc.* **1992**, *139*, 671. (b) Kamath, P. V.; Therese, G. H. A.; Gopalakrishnan, J. *J. Solid State Chem.* **1997**, *128*, 38. (c) Faure, C.; Delmas, C.; Fouassier, M. *J. Power Sources* **1991**, *35*, 279.

(17) (a) Watanabe, K.; Kikuoka, T.; Kumagai, N. *J. Appl. Electrochem.* **1995**, *25*, 219. (b) Elumalai, P.; Vasan, H. N.; Munichandraiah, N. *J. Power Sources* **2001**, *93*, 201. (c) Reichle, W. T. *Solid State Ionics* **1986**, *22*, 135. (d) Cao, L.; Xu, F.; Liang, Y. Y.; Li, H. L. *Adv. Mater* **2004**, *16*, 1853. (e) Terasaki, I.; Sasago, Y.; Uchinokura, K. *Phys. Rev.* **1997**, *B56*, R12685. (f) Kurmoo, M. *Chem. Mater.* **1999**, *11*, 3370. (g) Rujiwatra, A.; Kepert, C. J.; Claridge, J. B.; Rosseinsky, M. J.; Kumagai, H.; Kurmoo, M. *J. Am. Chem. Soc.* **2001**, *123*, 10584.

(18) Liu, Z.; Ma, R.; Osada, M.; Takada, K.; Sassaki, T. *J. Am. Chem. Soc.* **2005**, *127*, 13869.

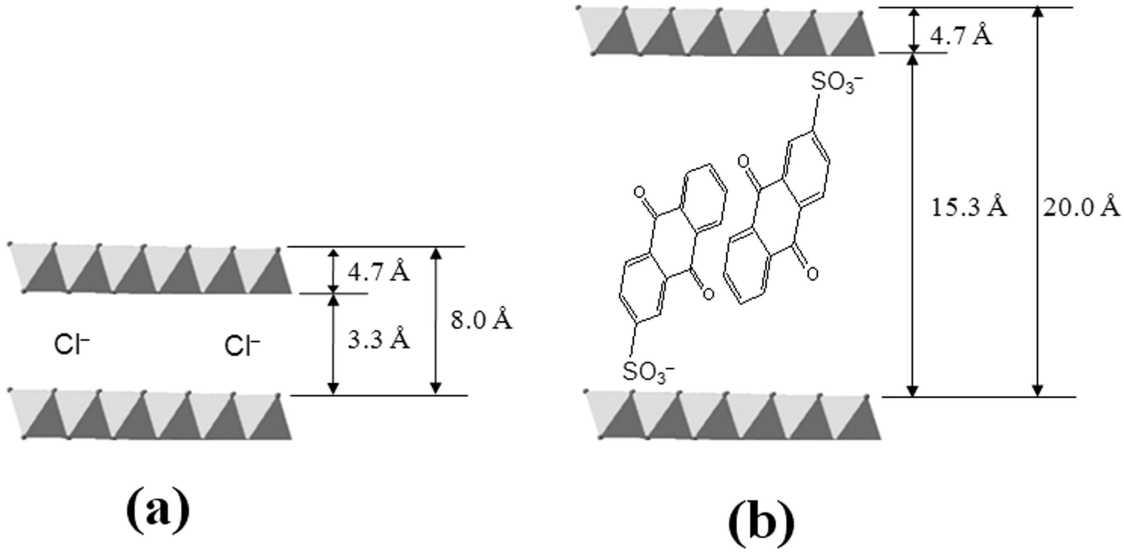

Figure 3. Schematic illustrations for the interlayer structures of (a) Cl- and (b) AQS2-α-$Co(OH)_2$.

poly(acrylic acid) (PAA) onto the Si substrate. The MUA and TMSPMA SAMs play a critical role as the organic interface in growing films. The terminal carboxylic acid group in this experiment can serve metal cation binding.

Experimental Details

All starting chemicals were purchased from Aldrich and used as received.

Surface Functionalization. The surface functionalization of a thin Au layer with of 11-mercaptoundecanoic acid (MUA) was accomplished by immersing the substrate (Au deposited on Si) in 1% (v/v) ethanol solutions of MUA for 3 h. The MUA/Au/Si sample was washed with ethanol and was dried with a stream of nitrogen. The silicon substrates were cleaned by a piranha solution for 1 h. The functionalization of the silicon surface by 3-(trimethoxysilyl)-propyl methacrylate (TMSPMA) was accomplished by immersing the silicon substrate in 1% (v/v) ethanol solutions of TMSPMA for 3 h. The TMSPMA/Si samples were washed with ethanol and were dried at 120 °C for 10 min in a dark room. The TMSPMA/Si substrate was treated with aqueous solution (20 mL) of potassium persulfate for 30 min at room temperature. Under vigorous stirring, the acrylic acid (AA) was then added and the mixture was placed in an oil bath at 75 °C for 30 min. After surface grafting polymerization of poly(acrylic acid) (PAA), the substrate was rinsed with ethanol in an ultrasonic bath for 5 min and dried with a stream of nitrogen.

Synthesis of X-Co-LDH Films (X = Cl or AQS2). The X-Co-LDH films (X = Cl or AQS2) were prepared by in situ crystallization on either the MUA/Au/Si or PAA/TMSPMA/Si substrate. The synthesis of the LDH films was performed in vials in air. For Cl-Co-LDH films, $CoCl_2 \cdot 6H_2O$, NaCl, and hexamethylenetetramine (HMT) were dissolved in 20 mL of a 9:1 mixture of deionized water and ethanol to give the final concentrations of 10, 10, and 60 mM, respectively. For AQS2-Co-LDH films, $CoCl_2 \cdot 6H_2O$, anthraquinone sulfonic acid (AQS2; anthraquinone-2-sulfonic acid sodium salt), and hexamethylenetetramine (HMT) were dissolved in 20 mL of a 9:1 mixture of deionized water and ethanol to give the final concentrations of 10, 10, and 60 mM, respectively. The reaction solution was then heated at about 75 °C with magnetic stirring. After growing the LDH films for about 12 h, the substrates were sonicated in ethanol for 5 min to remove physically absorbed particles and finally dried with a stream of nitrogen. To minimize the influence of colloidal precipitation, the functionalized surface of the substrate was placed facing down in the bath. A suspension containing green product was filtered and washed with deionized water and anhydrous ethanol several times and finally air-dried at room temperature.

Characterization. X-Ray diffraction (XRD) data were collected on a Philips PANalytical X'pert pro diffractometer with Cu Kα radiation from 3° to 70° with $\lambda = 1.542$ Å, 40 kV, 40 mA. Fourier transform infrared (FT-IR) spectroscopy spectra for powder were recorded on a Biorad FTS 6000 FT-IR spectrometer equipped with a high performance DuraSamplIR II diamond accessory of attenuated total reflectance (ATR) mode in the range of 400−4000 cm^{-1} with 100 scans at 4 cm^{-1} resolution and the photovoltaic liquid cooled mercury−cadmium−telluride (MCT) detector. FT-IR spectra for the film were recorded on the same spectrometer equipped with Pike Veemax specular reflectance accessory. An ellipsometer (Beaglehole Instruments) equipped with a He−Ne laser (632.8 nm) was used to determine the thickness of the TMSPMA and PAA films. Atomic force microscopy (AFM) measurements were performed in air with a Nanoscope III scanning probe microscope (Digital Instruments). The "E" scan head was used for a 10 μm maximum scan in tapping mode. Sharpened silicon tips with Al reflex coating on the detector side (force constant: 40 N m^{-1}, BudgetSensors) were used. Scanning electron microscopy (SEM) images were taken on JSM 840F at 25 kV. The samples were attached to a carbon holder and lightly coated with Pt/Pd to reduce surface charge. Voltametric measurements were made by using a potentiostat/galvanostat (Zahner, IM6). All electrochemical measurements were carried on a conventional three-electrode cell with a Pt disk counter electrode, a saturated Ag/AgCl reference electrode, and LDH/Au films as a working electrode. Electrolyte solutions (0.1 M PBS, phosphate buffered saline, of pH 7.5) were made using deionized water purified with a Millipore Milli-Q system (18 MΩ/cm). Cyclic voltammograms (CV) were measured under the potential sweep rate of 100 mV/s. N_2 saturation of the electrolyte was made for 3 h before the electrochemical measurements.

Results and Discussion

To facilitate nucleation and growth of the cobalt hydroxide crystalites on the Au and Si substrates, these surfaces were chemically functionalized. We aimed to generate a modified surface which was rich in carboxylic groups that could bind

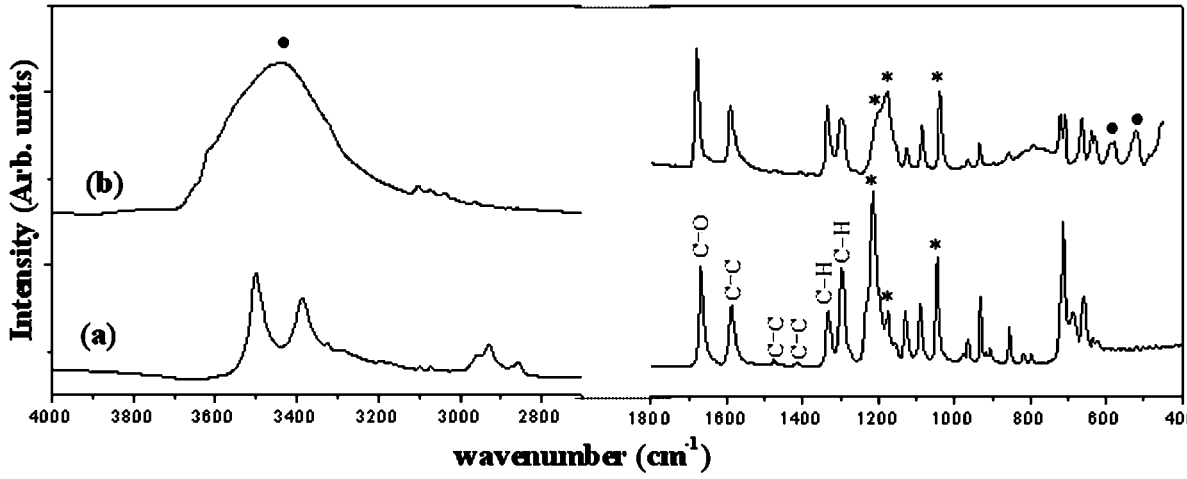

Figure 4. FT-IR spectra of (a) anthraquinone-2-sulfonic acid sodium salt (AQS2) and (b) AQS2-α-$Co(OH)_2$ thin film on MUA/Au/Si substrate. The dark circles correspond to LDH host layer, and the asterisks to sulfonate group of AQS2 anion.

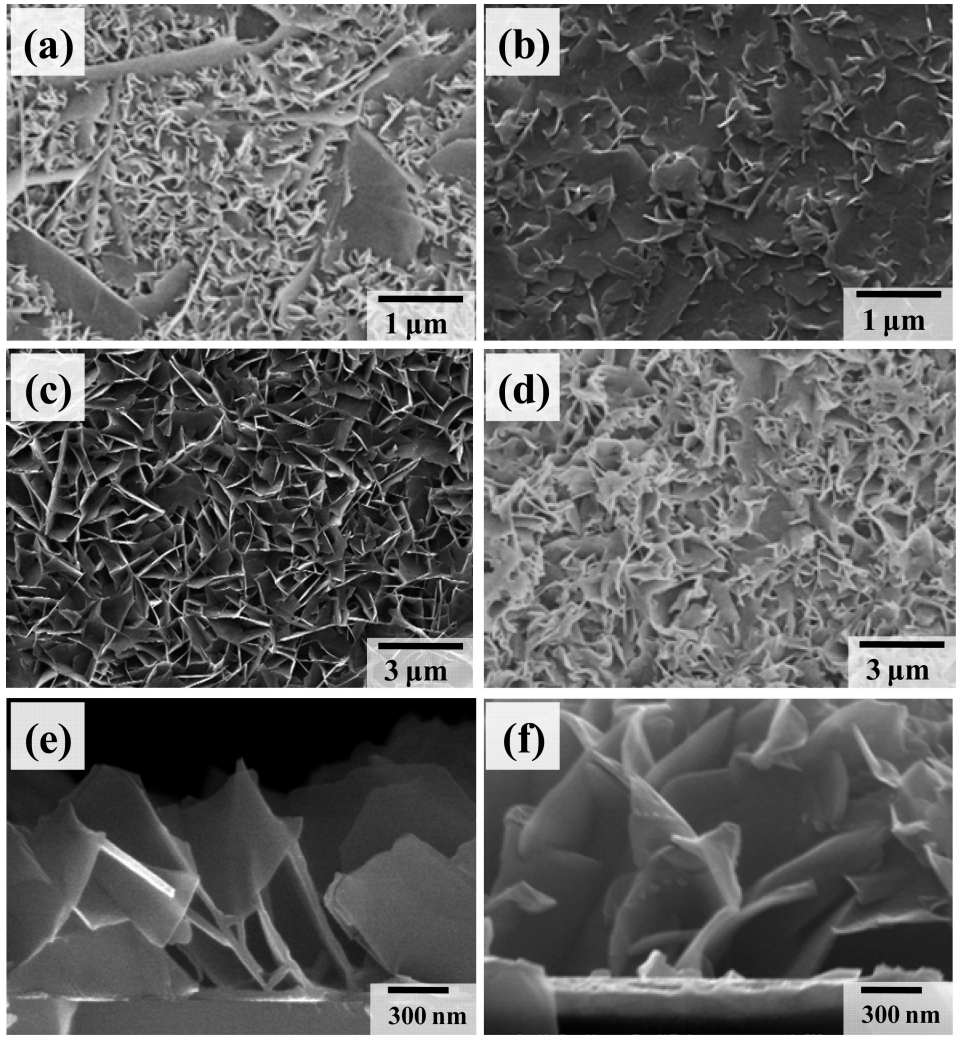

Figure 5. SEM images of Cl-α-$Co(OH)_2$ film on PAA/TMSPMA/Si (a) and on MUA/Au/Si (b) and AQS2-α-$Co(OH)_2$ film on PAA/TMSPMA/Si (c) and on MUA/Au/Si (d), respectively. Parts (e) and (f) are cross-sectional views of (c) and (d).

the Co^{2+} ions and so act as nucleation centers. Thus self-assembled monolayers (SAMs) of 11-mercaptoundecanioc acid (MUA) were formed on the gold surface by immersing a thin film Au substrate in an ethanolic solution of MUA. Thin films of poly(acrylic acid) (PAA) were successfully prepared on a 3-(trimethoxysilyl)propyl methacrylate (TMSPMA) functionalized Si substrate by in situ grafting polymerization of acrylic acid. To functionalize the Si surface by TMSPMA the Si surface was activated to produce surface hydroxyl groups. The surface morphology, roughness, and thickness were measured using both AFM and ellipsometry. The ellipsometry measurements demonstrate that the thick-

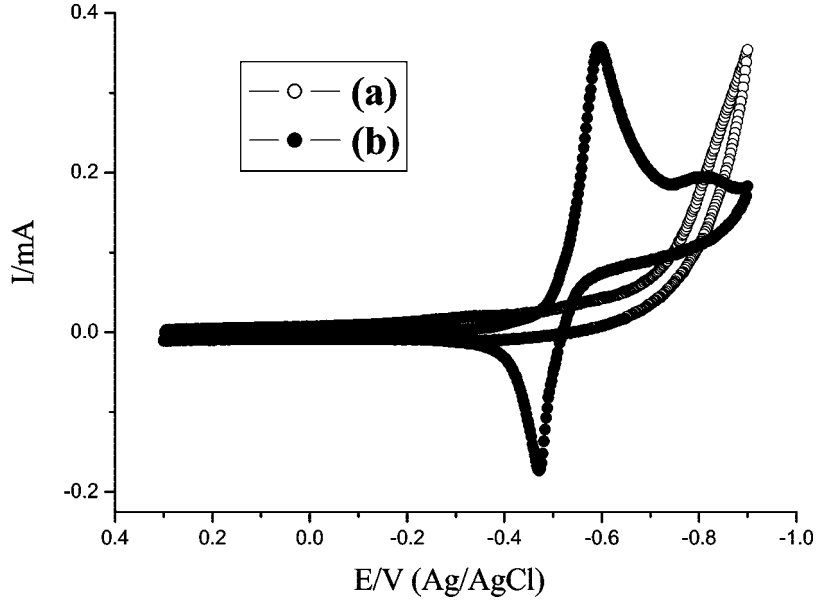

Figure 6. Cyclic voltammograms of (a) Cl-α-$Co(OH)_2$ and (b) AQS2-α-$Co(OH)_2$ thin films on MUA/Au/Si substrate. The electrochemical measurements were performed in deoxygenated 0.1 M PBS (pH 7.5) with a conventional three-electrode system including an Ag/AgCl reference electrode, a Pt counter electrode, and LDH/Au as a working electrode (υ = 100 mV/s).

Table 1. Cyclic Voltammetric Data for the AQS2-α-$Co(OH)_2$ Thin Film on a Modified Gold Substrate

scan rate (mV/s)	E_{Pc} (V)	I_{Pc} (mA/cm^2)	ΔE_P (mV)	$\lvert I_{Pc}/I_{Pa}\rvert$
20	−0.61	0.22	71	1.4
100	−0.59	0.36	120	2.1

nesses of TMSPMA and PAA thin films were 0.13 and 0.31 nm, respectively. The estimated thickness of perfect, close-packed SAMs of TMSPMA is about 1.2 nm assuming that the SAMs are perpendicular to the substrate surface.[19] The surface coverage of TMSPMA SAMs on the SiO_2 surface was approximately 11%. In densely packed SAMs of alkylsiloxanes on SiO_2 surface, the packing density is 4.67 molecules nm^{-2}.[19] Therefore, the packing density was about 0.5 molecules nm^{-2}. Figure 1c,d show the plan-view and three-dimensional AFM images of a PAA polymerized area of 1 μm × 1 μm. The rms roughness of the PAA thin film is approximately 0.16 nm, and grain size is around 60 nm. According to the AFM images and thickness measurement, the PAA thin film was successfully polymerized on the TMSPMA/Si surface.

Bulk samples of intercalated layered α-cobalt hydroxides can be directly synthesized by the homogeneous hydrolysis of $CoCl_2$ solution with HMT in the presence of an intercalating anion.[18] Both $Co(OH)_{2.04}(CO_3)_{0.03}Cl_{0.26}\cdot 0.32H_2O$ and $Co(OH)_{2.23}(CO_3)_{0.06}AQS2_{0.28}\cdot 0.68H_2O$ (see Supporting Information) can be prepared by this method by using NaCl or NaAQS2, respectively. Figure 2 shows the XRD data of the green product precipitated from $CoCl_2$ solution with HMT and AQS2. The XRD indicates a well-crystallized rhombohedral, hydrotalcite-like, $3R_1$ phase. The XRD pattern of the green precipitate may be indexed by using lattice parameters a = 3.11 Å and c = 60.00 Å. The lattice constants are similar to those found in Zn/Al-AQS2. The observed interlayer spacing of 20.0 Å gives an effective separation of 15.3 Å to accommodate the AQS2 anions (assuming a 4.7 Å thickness for the cobalt hydroxide layer[18]). Since AQS2 has a length of 12.9 Å,[20] an antiparallel arrangement of AQS2 anions is proposed, as shown in Figure 3.

The functionalized substrates were then placed in a solution containing $CoCl_2$, HMT, and the appropriate guest anion. After 12 h the substrates were sonicated in ethanol for 5 min to remove physically absorbed particles and finally dried with a stream of nitrogen. The layered structures that formed on the MUA/Au/Si and the PAA/TMSPMA/Si substrates were characterized by XRD, SEM, FT-IR, and electrochemistry. Thin films of α-cobalt hydroxide intercalated with Cl^- and AQS2 anions were obtained by a similar reaction condition with the functionalized substrates. The XRD data for α-cobalt hydroxide intercalated with Cl^- (Cl-α-$Co(OH)_2$) gives a interlayer spacing = ∼8 Å, which is in agreement with reported values.[18] The XRD data for the AQS-α-$Co(OH)_2$ thin films crystallized on the MUA/Au/Si the PAA/TMSPMA/Si substrates are shown in Figure 2. The XRD data for the AQS2-α-$Co(OH)_2$ thin films are very similar to that of the bulk sample.[20]

FT-IR Spectra. The FT-IR spectra in Figure 4 of AQS2-α-$Co(OH)_2$ exhibit the characteristic absorption features of α-cobalt hydroxide and the anthraquinone-2-sulfonate anion. The large broadband centered at 3500 cm^{-1} is assigned to overlapping stretching modes of hydroxyl groups present, both those in the brucite-type layer and the interlayer water molecules. The bands below 600 cm^{-1} are associated with Co−O stretching and Co−OH bending vibrations.[18]

The strong vibration band observed at around 1690 cm^{-1} is assigned to C═O stretching mode. The peaks at 1590, 1473, and 1413 cm^{-1} are assigned to C═C aromatic stretching mode and others at 1334 and 1300 cm^{-1} to C−H

(19) (a) Wasserman, S. R.; Tao, Y.-T.; Whitesides, G. M *Langmuir* **1989**, *5*, 1074. (b) Pale-Grosdemange, C.; Simon, E. S.; Prime, K. L.; Whitesides, G. M. *J. Am. Chem. Soc.* **1991**, *113*, 12.

(20) Kuk, W. K.; Huh, Y. D. *J. Mater. Chem.* **1997**, *7*, 1933.

aromatic stretching modes, respectively. The peaks at 1213 (broad), 1176, and 1037 cm^{-1} are attributed to asymmetrical and symmetrical stretching modes of interlayer sulfonate anion, respectively.[21] The S−O stretching bands of SO_3^- are shifted from 1213 (sharp, asymmetric mode) and 1045 cm^{-1} (sharp, symmetric mode) in the sodium salt to 1200 (broad) and 1037 cm^{-1} (sharp) in layered structure, respectively. The extremely reduced intensity of the asymmetric stretching mode due to the sulfonate groups indicates the intercalation of AQS anions into the hydroxide layers. Additionally, no absorbance due to carbonate anion intercalation is detected by FT-IR spectroscopy.

Morphologies and Electrochemistry. The morphologies of the as prepared α-$Co(OH)_2$ films were characterized using SEM. Figure 5a,b shows the top-view of Cl-α-$Co(OH)_2$ thin films on the PAA modified Si and MUA modified Au/Si substrates, respectively. For the PAA/Si substrate, a curved hexagonal face of cobalt hydroxides could be observed and covers almost the entire substrate. This morphology is similar to that of thin films of MgAl-LDH grown on a sulfonated polystyrene substrate.[13a] Some large hexagonal platelets may be deposited from the colloidal precipitates. In contrast, for the MUA/Au/Si substrate, the morphology of Cl-α-$Co(OH)_2$ thin film was smooth, and the platelets are disordered, which may be ascribed to the different packing density of the SPMP and the TMSPMA SAMs on Au and Si surfaces.[19,22] In the AQS anions system, the SEM images in Figure 5 c,d show that the substrates were entirely covered with large and thin microcrystals of 10−20 nm in thickness, and the platelets were randomly orientated but were attached by their edges to the surface and oriented perpendicular to the surface. The crystallite growth in AQS2-α-$Co(OH)_2$ thin films occurred much more faster than for the Cl-α-$Co(OH)_2$. Furthermore, the cross section view indicates that the cobalt hydroxide platelets grow oriented perpendicular to the substrate and interlock to form petal-like structures.

An electrochemical behavior of the hybrid thin films was investigated in aqueous solution of 0.1 M buffer (pH 7.5). Representative cyclic voltammograms for the AQS2-α-$Co(OH)_2$ and the Cl-α-$Co(OH)_2$ grown thin films on gold substrate were obtained from −0.9 to 0.3 V vs Ag/AgCl reference electrode by using conventional three electrode cell, as shown in Figure 6. In Cl-α-$Co(OH)_2$ system, no electrochemical event was detected in the applied potential range. The AQS2-α-$Co(OH)_2$ thin film exhibits an electrochemical response characteristic of the reversible redox process between AQS and AQS^{2-}. The cathodic peak current for the AQS anion incorporated in the interlayer is clearly observed at approximately −0.59 V vs Ag/AgCl, in which a half-wave potential[23] ($E_{1/2} = -0.575$ V) is almost in good accordance with the value of free AQS anions.[24] Table 1 shows actual electrochemical data observed at the different scan rates. The difference between anodic and cathodic peak potential ΔE_P and the $|I_{Pc}/I_{Pa}|$ can be related to the reversibility of the electron transfer.[24b] The difference of peak potential ΔE_P and the $|I_{Pc}/I_{Pa}|$ was increased from 71 to 120 mV and from 1.4 to 2.1, respectively, with increasing scan rate as shown in the Table 1. This behavior might be ascribed to the slow redox process or high resistivity of the LDH films.[24b,25] In addition, no additional electrochemical events are observed after soaking the hybrid films in the electrolyte solution for 1 h, indicating that the AQS anions incorporated between the $Co(OH)_2$ layers do not release into the electrolyte solution.

Conclusions

The thin films of α-$Co(OH)_2$ intercalated with anthraquinone-2-sulfonates have been grown on carboxylic acid modified Au and Si substrates by homogeneous hydrolysis of HMT. The MUA SAMs and PAA, polymerized from TMSPMA SAMs on Si substrate, were used as organic interface between hybrid thin films and substrates. Attempts to grow AQS2-α-$Co(OH)_2$ films on unmodified Si were unsuccessful. For AQS2-α-$Co(OH)_2$ hybrid film an antiparallel arrangement of the AQS2 ions is proposed. The electrochemical response for the AQS2-α-$Co(OH)_2$ film on MUA/Au/Si clearly indicates the complete incorporation of AQS anion species into the interlayer spaces. These hybrid organic-LDH thin films will provide several advantages such as improved mechanical adherence and stability usually difficult in colloidal deposition. Considering the advantages of LDHs, such as a large compositional variation and the high anion exchange capacity for a range of guest anions, the present technique is of great interest in the development of well-defined functional nanocomposite thin films and gas permeable membranes for specific applications.

Acknowledgment. This work was supported by the Korea Research Foundation Grant funded by the Korean Government (MOEHRD) (KRF-2006-352-C00039).

Supporting Information Available: Full XRD patterns, thermogravimetric analyses, and chemical analyses for powder samples (PDF). This material is available free of charge via the Internet at http://pubs.acs.org.

CM802828Z

(21) Moriguchi, T.; Yano, K.; Nakagawa, S.; Kaji, F. *J. Colloid Interface Sci.* **2003**, *260*, 19.
(22) Herrwerth, S.; Eck, W.; Reinhardt, S.; Grunze, M. *J. Am. Chem. Soc.* **2003**, *125*, 9359.
(23) Nicholson, R. S.; Shain, I. *Anal. Chem.* **1964**, *36*, 706.
(24) (a) Bechtold, T.; Gutmann, R.; Burtscher, E.; Bobleter, O. *Electrochim. Acta* **1997**, *42*, 3483. (b) Mousty, C.; Therias, S.; Forano, C.; Besse, J. P. *J. Electroanal. Chem.* **1994**, *374*, 63.
(25) Itaya, K.; Chang, H. C.; Uchida, I. *Inorg. Chem.* **1987**, *26*, 624.